QUANTITATIVE MEASUREMENTS IN VIBRO-ACOUSTOGRAPHY

A. L. Baggio*, H.A.S. Kamimura**,J. H. Lopes*, A.O. Carneiro** e G.T. Silva*

* Instituto de Física, Universidade Federal de Alagoas, 57072-900, Maceió-AL, Brazil.
**Departamento de Física, FFCLRP, Universidade de São Paulo, 14040-900, Ribeirão Preto, Brazil
e-mail: baggio@usp.br

Abstract:. Vibro-acoustography (VA) is an acoustic image modality based on the response of tissue under excitation of two ultrasound beams with different-frequencies. The aim of this paper is to provide a quantitative analysis with experimental measurements of the difference-frequency (DF) pressure generated in VA. This analysis considered the radiation force , the induced acoustic emission, and nonlinear wave mixing (parametric array and interaction of sound-with-sound). An experimental setup was devised employing a confocal ultrasound transducer driven by two sinusoidal signals at frequencies 3.2 ± f_ / 2 MHz, with f_ = 50, 60, 70, and 100 kHz, generating a pressure field over a metallic sphere placed at the transducer focus into a water tank. The DF pressure was measured as function of the distance *r* from the spherical target to an acoustic hydrophone placed along the transducer axis. The results showed the main contribution to the VA signal is due to the parametric array and the nonlinear scattering of sound-by-sound where the last one is responsible for the VA image contrast. The estimated acoustic emission and the linear scattering components had amplitudes less than -80dB of the detected signal. The statistical analyzes showed that the nonlinear decay model, which predicts a spatial variation $r^{-1}(1+\ln r)$, is more efficient to explain the experimental data (R_square>0.86) when compared with the acoustic emission theory model (r^{-1}), that presented poor correlation coefficients.

Keywords: Vibro-acoustography, Difference-frequency generation, Nonlinear wave mixing.

Introduction

Vibro-acoustography is an imaging method that employs at least two co-focused ultrasound beams above (1 MHz) to produce a difference-frequency (DF) pressure (with frequency smaller than 100 kHz), which is used to form an image of biological tissues [1]. The co-focused ultrasound beams are raster-scanned over the region of interest, where they mix and generate a time-series of the DF pressure that was detected by a sensitive hydrophone to form images.

Several promising *in vitro* VA studies have been performed to imaging kidney stones [2]; vibrational characteristics of bone fracture [3]; bones [4] and metal implants [4]. The VA implementation on a clinical ultrasound systems [5] with commercial transducers improved significantly the VA image quality allowing i*n vivo* clinical applications[6]. Although VA already established in the literature, the method is still based on qualitative analysis. Therefore, the next step to improve VA requires a better understanding of the quantitative aspects of the image formation process.

So far, the DF generation in VA has been explained in terms of two distinct phenomena. Initially, VA was modeled based on the time-modulated radiation force [7] exerted by the incident ultrasound beams on a suspended object. As a response to the time-varying force, the object is set in motion (i.e. it may move and/or deform). Subsequently, the object emits a pressure at the DF, the so-called acoustic emission. Based on this description, an imaging formation model for VA was proposed using the radiation force theory [8]. A later description of the DF generation in VA was made in terms of the nonlinear mixing of the primary scattered waves by inclusions in the medium [9].

In VA, the difference-frequency generated pressure can be expressed as

$$p_{-} = (p_{AE} + p_{PA} + p_{SP} + p_{SS})e^{-i\omega_{-}t}, \qquad (1)$$

where p_{AE} is the acoustic pressure emission induced by a time-harmonic radiation force[10], p_{PA} is the parametric array pressure of a dual-frequency focused beam [11], p_{SP} is the scattered parametric array pressure [12], and p_{SS} is the pressure yielded by the interaction of sound-with-sound phenomenon [13].

The previous theoretical results [14] show that only parametric array and interaction of sound-by-sound interaction have significant contribution in the VA detected signals. Thus, the aim of this paper is to present experimental evidence that the DF pressure amplitude is the combination of the parametric array and the interaction of sound-by-sound.

Materials and Methods

The physical phenomena responsible for the difference frequency generation in VA may be investigated by analyzing the decay of the low-frequency response of targets along the propagation path of the waves. In this investigation, we analyze the DF pressure decay with the axial distance as a result from the

scattering of the incident wave by a 1 mm-diameter tungsten carbide sphere excited by two co-focused ultrasonic beams.

Experimental apparatus – The ultrasonic beams were generated by a concave transducer composed by two-elements with inner radius of 14.8mm and outer ring spanning from 16.8 to 22.5mm with focus at 6.7 cm. The transducer was driven by two sinusoidal signals at 3.2 MHz ± *f*_/2, with *f*_ = 50, 60, 70, 100 Hz. A tone-burst of 100 ms with 0:3 % of duty-cycle applied to the driving signals to avoid undesirable reverberation. The signals were produced by two function generators (model 33120A, Agilent Technologies, Palo Alto, CA, USA) and amplified in 20 dB by a 2-channel-high-frequency-amplifier (homemade). The experiments were performed in a water tank with the metal sphere placed in the focus zone of the transducer. A hydrophone (model 8106, Bruel & Kjaer, Denmark)was moved by a motor-stepper positioning system (model TA-125u, Figlabs, Ribeirão Preto, São Paulo, BR) in the axial distance ranging from 8 to 18 cm away from the sphere with steps of 1 cm, this range correspond to typical distances used in main applications of VA. An oscilloscope (model MSO7104B, Agilent Technologies, Palo Alto, CA, USA) connected to the hydrophone output evaluated the average of 128 signals triggered by the tone-burst cycles of driving signals for each axial distance. To suppress the resonance response of the hydrophone, we subtracted the hydrophone's response of the medium The sound pressure magnitude computed for each of the signals was obtained b following a set of procedures. First we used a Hamming window to reduce the components of the envelope of signal later added a zero-padding = 1000 points to optimize the filtering process. Subsequently the resultant signal was filtered using 2nd order Butterworth digital bandpass filter with normalized cutoff frequencies at 95% and 105% of low frequency f_. The magnitude of the acoustic pressure value related to each position z, was calculated using the root mean square (RMS) of signals [24] . The shift due the changes in the target-detector distance are considered and the processing window (about 300 μs) was shifted to correct computation.

In the first experiment, the sphere was placed on the focus region and the DF signal was acquired. Keeping the same configuration, a second signal was obtained but now removing the sphere. In the second experiment, the signal was acquired with *f*_ = 0 to remove the background signal due the transducers rings. For all experiments, the incident pressure amplitude on focus was considered uniform and its value was measured using a needle hydrophone (model SN 1861, Precision Acoustics, Dorchester, UK) whose mean value on focus was 1.58MPa.

Nonlinear fitting - In this study, we consider two approaches to describe the behavior of the decay curve of the signal as a function of axial distance. In the first case named **(model 1)**, we assume a model based on acoustic emission pressure law. In the second one **(model 2)** the assumption is the nonlinear scattering sound-with-sound interaction is the main contribution in the detected signal whose simplified mathematical models can be described by:

model 1 :
$$p_{AE} = \frac{D_1}{r} \tag{2}$$

model 2 :
$$p_{SS} = C_1 \frac{\ln r}{r} + \frac{C_2}{r} \tag{3}$$

where D_1, C_1 and C_2 are constants that have pressure units and depend on primary incident beam and the acoustic properties of the particle. They can be estimated through a nonlinear fit method based on the root-mean square (RMS) value for the acquired time-series for each distance *r*.

The statistical goodness fit parameters for the models in (2) and (3) were obtained using the Levenberg-Marquardt nonlinear least-square method [16], which was coded in Matlab (The Mathworks Inc.). After fitting the data, a visual examination of the fitted curves and the goodness fit output parameters were used to evaluate each model can better explain the experimental data.

Results

Figure 1 shows two time series detected by the hydrophone. Fig. 1.a is the signal detected without the sphere and corresponds to the parametric array contribution. Fig. 1.b is the result of subtraction from the signal with sphere and the signal obtained in the absence of the sphere. In both cases, the background signal due the transducer ringing was removed from the original signal resulting in clearer signal.

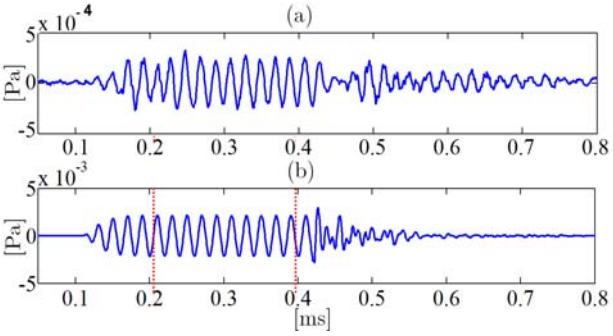

Figure 1 -The detected time series at difference frequency at f_ = 50 kHz. (a) The signal without the sphere (b) signal with sphere but subtracting the first signal (1a). The vertical dashed lines indicate the gate used to compute the RMS pressure.

Figure 2 shows the axial amplitude of parametric array computed by the Ding's algorithm [11] and the RMS values of the experimental data acquired without the sphere. To the experiments with the scatter (sphere), the signal contains the scattering pressure fields whose RMS values are shown in Figure 3. In the same figure, we include the nonlinear fitting to both decay models.

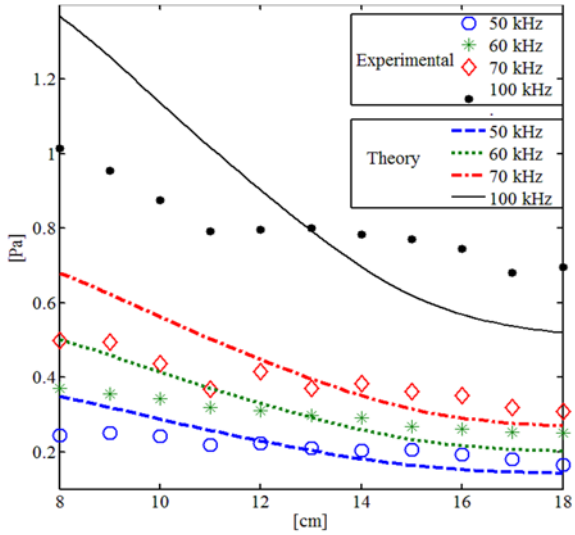

Figure-2 Parametric array pressure obtained for four difference-frequencies. The lines represent the parametric array pressure computed with Ding's algorithm [11].

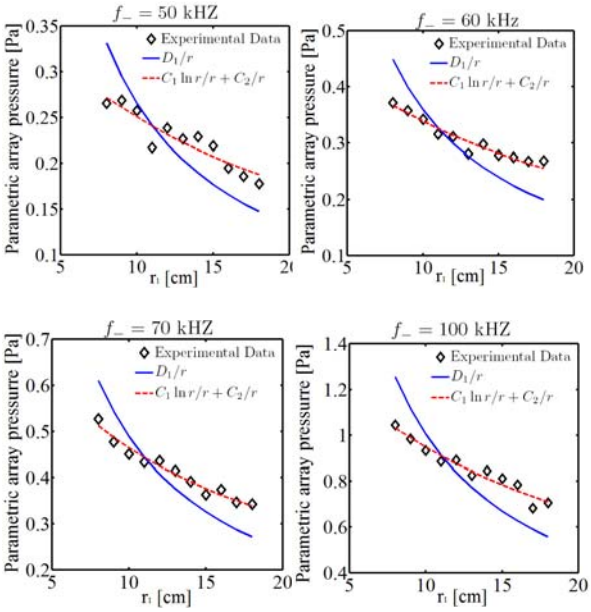

Figure 3- Decay curves obtained from the fitting procedure using the Nonlinear Least Squares Method non robust and Levenberg-Marquardt algorithm to experimental data for both models.

From the nonlinear fitting of both decay curve models, we could obtain the goodness fitting parameters showed in the table 1.

Table 1- The goodness of fit parameters obtained to both models (with 95% confidence bounds).

	Model 1		Model 2	
*f_* [kHz]	SSE	R-square	SSE	R-square
50	0.0125	-0.3032	0.0013	0.8630
60	0.0221	-0.6313	0.0008	0.9350
70	0.0318	0.0444	0.0011	0.9667
100	0.1649	-0.3657	0.0068	0.9441

Negative values of the correlation coefficient indicate a reverse type correlation, which is not in agreement with the theoretical decay models. Furthermore. Model 1 showed small values of negative correlation, indicating that this model is unable to explain the experimental data.

Discussion

The acoustic signal presented in the Fig 1.b can be associated with the contrast in the VA images, witch in the specific case the signal is about 10% of the parametric array contribution. The previous theoretical results [14] show that only the sound-by-sound interaction have significant contribution in the contrast in VA images. Computing the acoustic emission and the linear scattering of parametric array field components, we found no significant values (in order to -80 dB and -93 dB of main signal respectively) to this configuration. Thus, only the nonlinear p_{SS} component can be associated with VA image contrast.

Analyzing the RMS of signals detected without the sphere (figure 2), for different source/detector distances we found a fair agreement with the theoretical parametric array model, which was expected, since the scattering components are not present in any significant way. The oscillating pattern present in the four low frequencies and most strongly at f_=100 kHz can be explained due the experimental data can be understood in terms of the finite size of the hydrophone, while in Ding's algorithm the hydrophone is assumed to be a point detector.

When comparing the decay models through the nonlinear fitting we found, from a visual inspection, that the **model 2**, (nonlinear scattering)_fits better for all values of the difference-frequency *f_*. Furthermore, taking into account the values of SSE and R-square shown in Table 1, we notice that the nonlinear scattering **model 2** is the best to explain the experimental data. Moreover, considering the amplitude of the measured DF pressure, we observe a nonlinear relationship with respect to the frequency *f_*, which cannot be explained by the linear relation assigned to the acoustic emission model.

Conclusion

In the present work, we experimentally investigated the difference-frequency signal dependence as function of the radial distance from the scatterer (sphere) to the acoustic detector. The results indicate that the main contribution to the DF signal comes from the parametric array pressure and the scattering of sound- by-sound effect. Statistical analysis supports this conclusion. Thus, the nonlinear effects of acoustic scattering are more appropriate to explain the VA image contrast at different distances from the sample/detector. In addition, these results can help developing quantitative imaging techniques based on VA systems.

Acknowledgements

This work was partially supported by grants 481284/2012-5 and 303783/2013-220 3 CNPq (Brazilian agency), and by the São Paulo Research Foundation (FAPESP) under grant 2011/10809-6. The opinions, assumptions, and conclusions or recommendations expressed in this material are those of the authors and do not necessarily reflect the views of FAPESP.

References

[1]Fatemi M, Greenleaf J F. Ultrasound-stimulated vibro-acoustic spectrography. Science. 1998; 280(5360), 82-85.

[2] Mitri F G, Kinnick R R. Vibroacoustography Imaging of Kidney Stones In Vitro. IEEE Transactions on Biomedical Engineering. 2012; 59, 248-254.

[3] Alizad A, Wallch M, Greenleaf J F, Fatemi M. Vibrational characteristics of bone fracture and fracture repair: Application to excised rat femur. Journal of Biomechanical Engineering-Transactions of the Asme. 2006; 128, 300-308.

[4] Kamimura H A, Urban M W, Carneiro A A, Fatemi M, Alizad A. Vibro-acoustography beam formation with recon gurable arrays Ultrasonics, IEEE Transactions on Ultrasonics, Ferroelectrics and Frequency Control. 2012; 59(7), 1421-1431.

[5] Urban M W, Chalek C, Kinnick R R, Kinter T M, Haider B, Greenleaf J F, Thomenius K E, Fatemi M. Implementation of vibro-acoustography on a clinical ultrasound system Ultrasonics. IEEE Transactions on Ultrasonics, Ferroelectrics and Frequency Control. 2011a; 58(6), 1169-1181.

[6] Alizad A, Urban M W, Morris J C, Reading C C, Kinnick R R, Greenleaf J F, Fatemi M. In vivo thyroid vibro-acoustography: a pilot study. BMC medical imaging. 2013; 13(1), 1-13.

[7] Silva G T, Chen S, Greenleaf J F, Fatemi M. Dynamic ultrasound radiation force in fluids. Physical Review E. 2005; 71(5), 056617-1-9.

[8] Fatemi M & Greenleaf J F. Vibro-acoustography: An imaging modality based on ultrasound-stimulated acoustic emission. Proceedings of the National Academy of Sciences. 1999; 96(12), 6603-6608.

[9] Silva G T. Mitri F G. Difference-frequency generation in vibro-acoustography. Physics in medicine and biology. 2011; 56(18), 5985-5593.

[10] Silva G T, Chen S,Viana L P. Parametric amplification of the dynamic radiation force of acoustic waves in fluids. Physical review letters. 2006; 96(23), 234-301.

[11] Ding D. A simplified algorithm for the second-order sound fields. The Journal of the Acoustical Society of America. 2000; 108(6), 2759-2764.

[12] K.G. Foote, D.T.I. Francis P A. Calibration sphere for low-frequency parametric sonars. J. Acoust. Soc. Am.. 2007; 121, 1482-1490.

[13] Dean III L W. Interactions between sound waves. The Journal of the Acoustical Society of America. 1962; 34, 1039-1044.

[14] Silva G T, Bandeira A. Difference-frequency generation in nonlinear scattering of acoustic waves by a rigid sphere. Ultrasonics. 2013; 53(2), 470-478.

[15] Kenney J F, Keeping E S. Mathematics of Statistics, part 2. van Nostrand Princeton, NJ. 1962.